

Conditions for the abrupt bifurcation to chaotic scattering

Tamás Tél

Institute for Theoretical Physics, Eötvös University, Puskin u. 5-7, H-1088 Budapest, Hungary

Celso Grebogi^(a) and Edward Ott^(b)

Laboratory for Plasma Research, University of Maryland, College Park, Maryland 20742-3511

(Received 16 August 1993; accepted 4 October 1993)

One of the generic ways in which chaotic scattering can come about as a system parameter is varied is the so-called “abrupt bifurcation” in which the scattering is nonchaotic on one side of the bifurcation and is chaotic and hyperbolic on the other side. Previous work demonstrating the abrupt bifurcation [S. Bleher *et al.*, Phys. Rev. Lett. **63**, 919 (1989); Physica D **46**, 87 (1990)] was primarily for the case where the scattering potential had maxima (“hilltops”) which had locally circular isopotential contours. Here we extend these considerations to the more general case of locally elliptically shaped isopotential contours at the hilltops. It turns out that the conditions for the abrupt bifurcation change drastically as soon as even a small amount of noncircularity is included (i.e., the circular case is singular). The illustrative case of scattering from three isolated potential hills is dealt with in detail. One interesting result is a simple geometrical sufficient condition for an abrupt bifurcation in the case of large enough ellipticity of the hill with lowest potential at its hilltop.

I. INTRODUCTION

Chaotic scattering has attracted recent interest from various fields of science (for reviews see Refs. 1–4). An essential, and perhaps the simplest, class of problems exhibiting this phenomenon is provided by the class of potential scattering in which the trajectories are in an unbounded phase space and the motion of particles (whose mass can always be chosen to be unity) is governed by a potential $V(\mathbf{r})$.

Typically, whether the scattering process is chaotic depends on a system parameter, e.g., on the particle energy E . In two-degree-of-freedom cases there are two generic routes to chaotic scattering as a system parameter is changed:^{5–8} a sequence of saddle-center and period doubling bifurcations or a transition called an *abrupt bifurcation*.

In the case of an abrupt bifurcation, a chaotic set is created by a sudden change in the topology of the phase space accompanied by a sudden change in the scattering process as the energy E falls below a critical value. The critical value E_c is a local maximum of the potential energy function $V(\mathbf{r})$. An important feature of this scenario is that the chaotic set created at the bifurcation is *hyperbolic* and structurally stable. Thus there must exist a whole *interval* of energy values $E_0 < E < E_c$ in which the dynamics on the chaotic set can be encoded by symbol sequences containing combinations of a low number, m , of letters. The fact that the dynamics is structurally stable in some range is significant because it implies that no bifurcations annihilating or creating periodic orbits can occur. Such a situation has been called fully developed chaotic scattering.⁵ One can

then also be sure that, for $E_0 < E < E_c$, KAM tori or marginally stable periodic orbits do not exist and the topological entropy is constant. (In the energy range $E < E_0$ pruning may gradually set in together with the appearance of stable trajectories surrounded by KAM tori.)

In the range of fully developed chaotic scattering: $E_0 < E < E_c$, methods relying on the nice scaling properties of hyperbolic systems can be applied. If the energy is close to the critical value, the Lyapunov exponent on the strange set turns out to be proportional to $|\ln(E_c - E)|$, while the fractal dimension and the average lifetime of chaotic orbits^{5,9} are proportional to $|\ln(E_c - E)|^{-1}$. This shows that right after its appearance, the chaotic set is extremely unstable and sparse. It becomes denser and less repelling as the energy is lowered. As $(E_c - E)$ increases further, the logarithmic rule breaks down, but there are rapidly converging methods (like the periodic orbit sum^{10,11} or the analysis of the time delay function in the spirit of the thermodynamical formalism¹²) which provide us with highly accurate characteristics of the scattering process.

It is, therefore, of great interest if we can decide on the basis of knowledge of the potential $V(\mathbf{r})$ whether the chaotic scattering right after its onset is hyperbolic, i.e., whether an abrupt bifurcation occurs. In the case of potentials with circularly symmetric hilltops the question has been answered.⁵ For three unequal hills with maxima $E_{m_1} < E_{m_2} < E_{m_3}$ an abrupt bifurcation occurs as E drops below $E_c \equiv E_{m_1}$ if the hills are arranged as in Fig. 1 and the spatial extent of the hills is small compared to their separation [i.e., $V(\mathbf{r})$ rapidly approaches zero away from the maxima and we say that the hills are “isolated” in this case]. It is worth briefly recalling the argument leading to this result: the scattering from an isolated circularly symmetric hill can only produce a maximum deflection angle of $\pi/2$ as E approaches the value of the potential at the hilltop from above. As soon as E falls below the hilltop

^{a)} Also at Department of Mathematics and Institute for Physical Science and Technology.

^{b)} Also at Department of Electrical Engineering and Department of Physics.

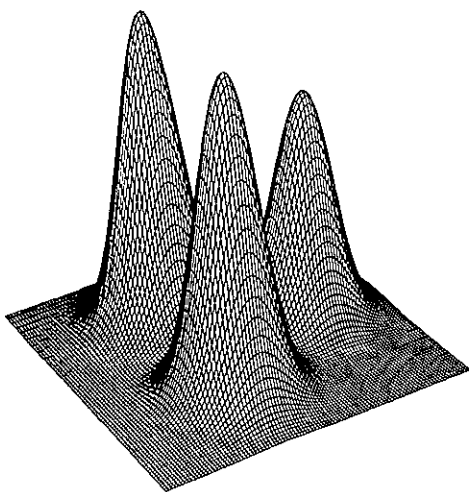


FIG. 1. Configuration leading to abrupt bifurcation in the case of three circularly symmetric potential hills.

value, a complete backscattering becomes possible and the deflection angle can take on any value between zero and π (depending on the impact parameter). Thus, for $E > E_{m_1}$, and the configuration of Fig. 1, when a trajectory comes from hill 2 or 3 toward hill 1, it cannot be reflected back to hills 2 and 3, since this would require a deflection angle bigger than $\pi/2$. Hence the only periodic orbit that can exist is the one bouncing between hills 2 and 3, and so there is no chaos when $E > E_{m_1}$. When E drops below E_{m_1} , chaos is immediately created since now the deflection angles required are possible, and this leads to the appearance of an infinity of periodic orbits, and these periodic orbits can be encoded by the order in which they visit the three hills.

While the example of Fig. 1 is for three isolated circularly symmetric hills, from the analysis of Ref. 5(b) it is clear that no qualitative change is to be expected if the hills are not globally circularly symmetric but the hilltops are locally circularly symmetric. That is, near a hilltop, $\mathbf{r} = \mathbf{r}_i$, the first two terms of the Taylor series expansion for the potential are of the form

$$V(\mathbf{r}) = V(\mathbf{r}_i) - K[(x - x_i)^2 + (y - y_i)^2] + O(r^3), \quad (1)$$

where K is a positive constant. Thus, isopotential contours $V(\mathbf{r}) = V_*$ are circular to lowest order in $V(\mathbf{r}_i) - V_* > 0$. In Ref. 5(b) the more general situation of locally elliptical isopotential contour near the hilltops [i.e., where the quadratic terms in the Taylor expansion of $V(\mathbf{r})$ are not of the restricted form above] was briefly discussed, and it was shown that major qualitative changes from the locally circular case can be anticipated.

Our aim in the present paper is to study a generic smooth repulsive potential whose isopotential contours are locally elliptical, rather than circular at the hilltops. In particular, we concentrate on the example of two-dimensional (x, y) scattering from three isolated potential hills where the hill of lowest hilltop potential is elliptically symmetric. The main problem we address is whether one

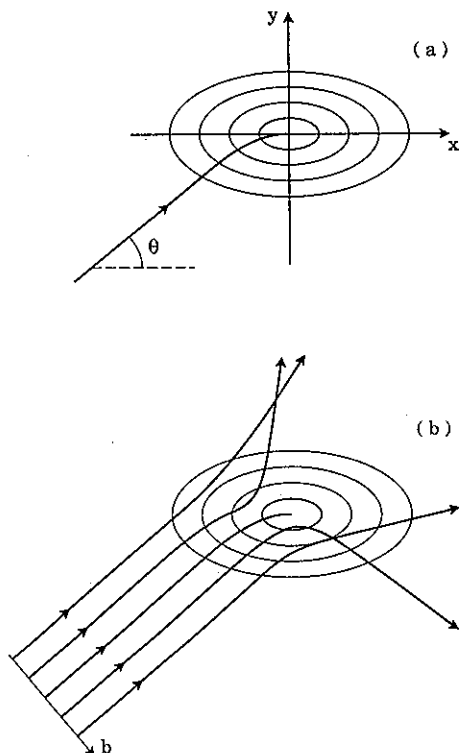


FIG. 2. Illustration of a critical trajectory reaching the hilltop in an infinitely long time for an elliptically shaped potential hill at $E = E_m + 0^+$ where E_m is the hilltop value.

finds a criterion relying solely on the geometrical configuration of the hills (in a similar way for an abrupt bifurcation as in Fig. 1). The essential novel feature^{5(b)} is that the absence of rotation symmetry leads to a completely new scattering behavior even for one isolated hill. As Fig. 2 illustrates, in the limiting case $E \rightarrow E_m + 0^+$, the trajectories can reach the hilltop along the major axis only. Consequently, it can be shown that they leave the hilltop along the minor axis (where the force is the strongest) in the positive or negative y -direction (Sec. II). By defining the deflection angle ϕ as the modulus of the angle between the incident and outgoing velocity, we see that there must be a jump from a scattering angle of $\pi/2 - \theta$ to one of $\pi/2 + \theta$ as the initial condition moves from the left side to the right side of the critical trajectory depicted in Fig. 2. This occurs at any deviation from circularity. Because of the strong anisotropy, the actual condition for abrupt bifurcation generally will depend on the details of the potential. For the example we consider, it will be shown, however, that the situation becomes simpler for sufficiently elongated potential forms. We shall show that in this class, if both hills 2 and 3 lie closer to the line of the major axis of hill 1 than some critical angle θ_c of order unity, then scattered trajectories always leave the potential toward the other side of the major axis for $E \rightarrow E_{m_1} + 0^+$; consequently, no chaos is present as long as $E > E_{m_1}$, and at E_{m_1} an abrupt bifurcation occurs (Secs. III and IV). In other cases when the hills are farther away from the major axis, or when the potential is not strongly elongated, we find that an abrupt

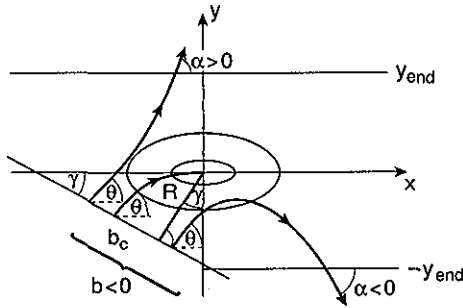


FIG. 3. Diagram illustrating scattering trajectories in the case of an infinitely extended elliptically shaped potential hill at $E = E_m + 0^+$. Trajectories are launched toward the hill along a straight line making angle γ with the x -axis under inclination angle θ . The impact parameter b is the distance of the initial point measured along this line from its intersection with the y -axis. $b_c < 0$ denotes the impact parameter of the critical trajectory. R is the distance of the initial line from the origin. The deflection angle ϕ is defined by measuring the direction α of the velocity when the trajectory crosses the line $y = y_{\text{end}} > 0$ ($y = -y_{\text{end}}$) in the case of forward (backward) scattering and taking $\phi = |\alpha - \theta|$.

bifurcation may still occur, but the particular condition for it to occur has to be worked out case by case. We illustrate by examples how this can be done (Sec. V). The paper ends with some concluding remarks (Sec. VI).

II. SCATTERING ON AN INFINITELY EXTENDED ELLIPTICAL POTENTIAL HILL

Whether the scattering process in the potential of three isolated hills with maxima $E_{m_1} < E_{m_2} < E_{m_3}$ can undergo an abrupt bifurcation depends (just like in the circularly symmetric case) on the capability of the hill with smallest maximum to deflect trajectories coming from the other hills toward any of the other hills when $E \rightarrow E_{m_1} + 0^+$.

Thus, we must first understand the scattering on a single isolated elliptically shaped potential hill. After rescaling, we can write the potential in the vicinity of the hilltop in the form

$$V(x, y) = E_m - \frac{1}{2}(x^2 + \beta^2 y^2), \quad (2)$$

where, without loss of generality, we can assume that $\beta > 1$. We thus choose the y -axis to be the direction of the strongest gradient and the x -axis to contain the major semiaxis of the isopotential contours. For specificity we consider in this section and in the next section (Sec. III) the behavior in the simple potential given by Eq. (2). That is, we take Eq. (2) to apply not only as an approximation near the origin, but as the exact potential everywhere. Following that, in Sec. V, we use the results of Secs. II and III, to obtain the conditions for abrupt bifurcations for the special case where the potential of the hill of lowest hilltop potential is given by Eq. (2) inside the contour $\frac{1}{2}(x^2 + \beta^2 y^2) = E_m$ and $V(x, y) = 0$ outside this contour.

We imagine that we inject particles along a straight line intersecting the x -axis with an angle γ which is considered to be positive in the configuration shown in Fig. 3. The inclination angle for the velocity of all the incoming particles is assumed to be the same value, $\theta > 0$, and the

total energy E is kept constant. If the particle leaves the potential in the upper half-plane (forward scattering), the deflection angle ϕ is observed along a line $y = y_{\text{end}} > 0$. In the case of a backscattering, the deflection angle is read off when the trajectory crosses the line $y = -y_{\text{end}}$. Denoting the angle between the trajectory and one of these straight lines by α , the deflection angle is simply $\phi = |\alpha - \theta|$.

When changing the position of the initial line, it is worth considering straight lines having the same distance R from the origin. By defining the impact parameter b as the distance of the initial position from the intersection of the straight line with the y -axis, the initial coordinates (x_0, y_0) are parametrized as

$$x_0 = b \cos \gamma, \quad y_0 = -\frac{R}{\cos \gamma} - b \sin \gamma, \quad (3)$$

where b is considered to be positive if the initial point lies to the right of the y -axis.

Since the force acting on the particle is linear in x and y , the motion can be described exactly, and an explicit form of the deflection function can be found. To see this, we recall that the solution to the Newtonian equations of motion in potential Eq. (2) is

$$x(t) = Ae^t + Be^{-t}, \quad y(t) = Ce^{\beta t} + De^{-\beta t} \quad (4)$$

with

$$A = (x_0 + v_{0x})/2, \quad B = (x_0 - v_{0x})/2, \\ C = (y_0 + v_{0y}/\beta)/2, \quad D = (y_0 - v_{0y}/\beta)/2. \quad (5)$$

In terms of the inclination angle,

$$\frac{v_{0y}}{v_{0x}} = \tan \theta = \text{const}, \quad (6)$$

and energy conservation implies

$$E = E_m - \frac{1}{2}(x_0^2 + \beta^2 y_0^2) + \frac{v_{0x}^2}{2 \cos^2 \theta}. \quad (7)$$

The last two relations can be used to eliminate the initial velocities from the coefficients A, \dots, D . Thus, the trajectories uniquely depend on the impact parameter b . Introducing $z \equiv \exp(\beta t)$ as a new variable, we immediately obtain the equation $x(y)$ of trajectories parametrized by z in the form of

$$x(y) = Az(y)^{1/\beta} + Bz(y)^{-1/\beta}, \quad z(y) = \frac{y \pm (y^2 - 4CD)^{1/2}}{2C}. \quad (8)$$

The sign in $z(y)$ must correspond to the sign of the initial velocity for $z \rightarrow 1$. As we always start trajectories with positive velocities, the plus sign is to be taken. In the case of backscattering, there is, however, a maximum of y , where the discriminant of $z(y)$ vanishes. There one has to go over to the other branch of the solution; i.e., where the y -coordinates decrease along the trajectory, the solution with the minus sign is valid. We note that an analogous expression exists for $y(x)$. Since, however, we are interested in trajectories with a given end point in y , the use of Eq. (8) is more convenient.

By taking the derivative of $x(y)$, the slope $\alpha = \arctan(y'/x')$ of a trajectory at coordinate y is easily obtained as

$$\alpha(y) = \arctan \left(\frac{\pm \beta (y^2 - 4CD)^{1/2}}{Az(y)^{1/\beta} - Bz(y)^{-1/\beta}} \right), \quad (9)$$

where C, D and $z(y)$ are given by (5) and (8), respectively. The deflection angle ϕ of a trajectory with end point $(x(\pm y_{\text{end}}), \pm y_{\text{end}})$ is

$$\phi = |\alpha(\pm y_{\text{end}}) - \theta| \quad (10)$$

where the sign of the end point coordinate is $+$ ($-$) for forward (backward) scattering. By substituting relations (3)–(9) into Eq. (10), one obtains an expression for the deflection angle as a function of the impact parameter b which can easily be plotted. Parametrically it depends for a given potential on the particle energy E , the inclination angle θ , and on the dimensionless ratio of the initial line distance R and the end point coordinate y_{end} . In our plots of the deflection function (Figs. 4, 5 and 9) we took initial conditions on the line $y = y_0$ which corresponds in the general notation to a case with $\gamma = 0, R = -y_0$, and $y_{\text{end}} = -y_0$. The deflection function then depends on β, E and θ only.

Let us first discuss the case $E = E_m + 0^+$ when the particle energy reaches the hilltop maximum from above. Denoting the impact parameter of the critical trajectory that asymptotes to the hilltop by b_c (see Fig. 2), we introduce the relative impact parameter δ measured from b_c via the relation $b = b_c \delta$. For negative values of δ , trajectories always intersect the line $y = y_{\text{end}} > 0$ (i.e., forward scattering is present). In the limit $\delta \rightarrow 0^-$, the trajectory will move toward infinity along the positive y -axis, and have a deflection angle $\pi/2 - \theta$. For small positive impact parameters δ , however, trajectories are reflected back by the hill and intersect the line where they started from. A trajectory with $\delta = 0^+$ comes back exactly along the negative y -axis and possesses a deflection angle $\pi/2 + \theta$. Thus, there is a *jump* of size 2θ at $\delta = 0$ so that the sum of the angles is always π which can clearly be seen in Fig. 4. Trajectories with small positive δ all intersect the line $y = -y_{\text{end}} < 0$ at positive x . Their α are thus less than $\pi/2$, and $\phi(\delta)$ is a monotonic decreasing function for δ positive. Increasing the impact parameter further, at a relatively large value of δ , the trajectory becomes asymptotically parallel to the x -axis, and thus $\alpha = 0$ (corresponding to $\phi = |\alpha - \theta| = |\theta|$). This marks the end point of the impact parameter interval with backscattering. One can show that the graph of $\phi(\delta)$ exhibits at this point an infinite slope [e.g., around $\delta \approx 1.7$ in Fig. 4(c)]. For larger values of δ forward scattering sets in again leading to a further decrease of the deflection angle.

One of the most striking features of the deflection function for noncircular potentials, $\beta \neq 1$, is that it can develop a *local maximum* lying higher than $\pi/2 - \theta$ at *negative values of δ* . If such a maximum is not present, all trajectories leave the potential with $x > 0$, i.e., the potential has a kind of “focusing” property. As long as the eccentricity of the isopotential contours is small, β is close to 1, the existence of a maximum follows from the fact that $\phi(\delta)$ must

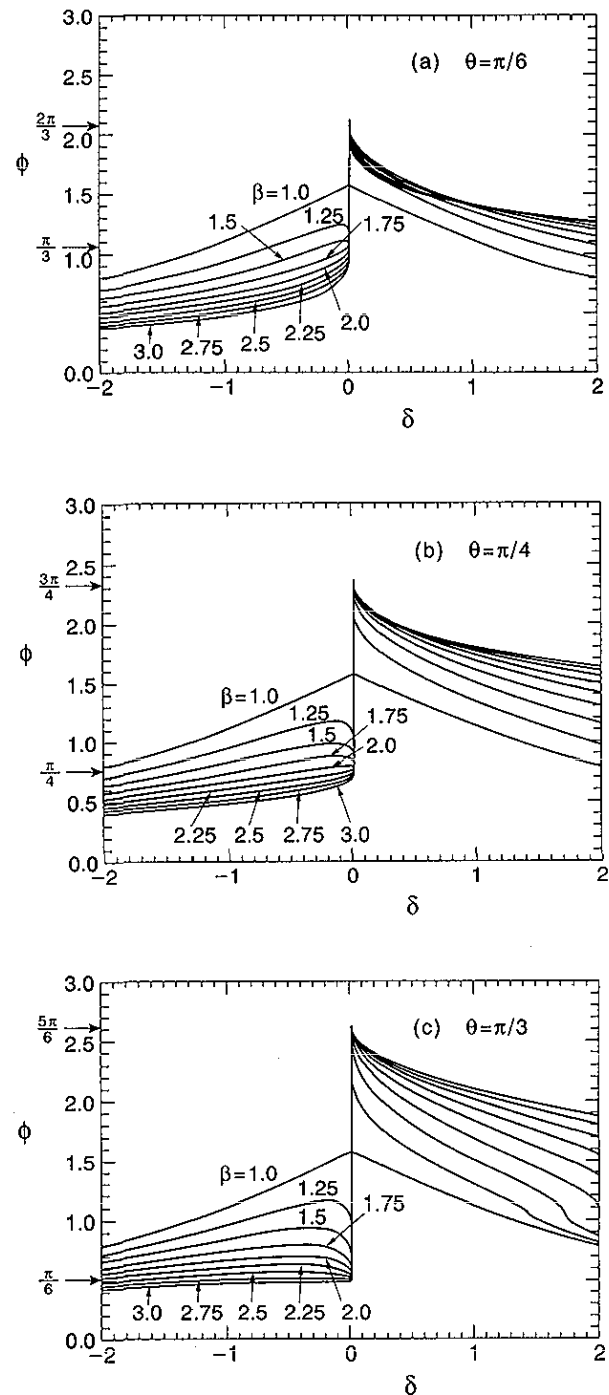


FIG. 4. Deflection function $\phi(\delta)$ where $\delta = b - b_c$ of infinitely extended potential hills at $E = E_m + 0^+$ as obtained from Eqs. (9) and (10) for different elongation parameters $\beta = 1.0, 1.25, 1.5, \dots, 3.0$ at incident angles: $\theta = \pi/6$ (a), $\theta = \pi/4$ (b), and $\theta = \pi/3$ (c). The initial line was chosen to be a horizontal one $y = -R = -y_{\text{end}}$, with $\gamma = 0$.

be close to the result of the circular case for δ not too small. An order unity deviation from the circular case is then restricted to a narrow range around $\delta = 0$ as discussed in Ref. 5. The diagrams of Fig. 4 show that local maxima are present at β values considerably different from unity, too, located at finite values of δ . Interestingly, the case $\beta = 2$ is a kind of boundary: one sees that for $\beta > 2$ (i.e., for sufficiently anisotropic hills) $\phi(\delta)$ can be monotonically

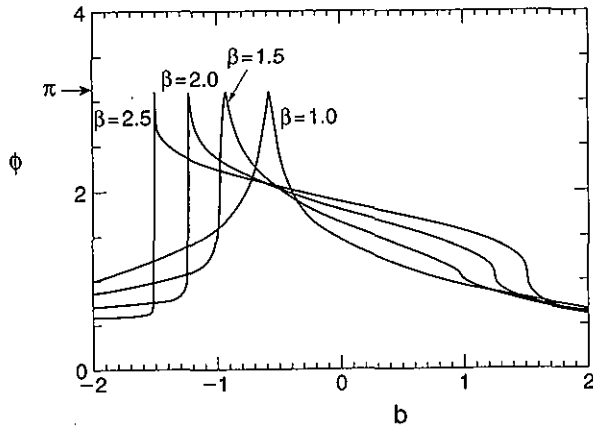


FIG. 5. Deflection function $\phi(b)$ of infinitely extended potential hills at $E=E_m-0.1$ as obtained from Eqs. (9) and (10) for different elongation parameters. Note that the value of $\phi=\pi$ is no longer excluded and implies complete backscattering. The initial line is the same as in Fig. 4.

decreasing as $|b|$ increases, and the above-mentioned “focusing” property is present. This behavior is, however, characteristic for a range of incident angles only. Figure 4(c) indicates that for $\theta=\pi/3$ a local maximum above $\pi/2-\theta$ can show up at negative δ . A careful analysis of the small δ limit, carried out in the next section, shows that this can never occur for θ values smaller than a critical value θ_c of order unity if $\beta > 2$, but does occur for potential shapes closer to circularity even for small incident angles [see Fig. 4(a)]. Thus, if the hill is sufficiently elongated, $\beta > 2$, and the incident direction is sufficiently close to the x -axis, $\theta < \theta_c$, all scattering trajectories end in the half-plane $x > 0$. This “focusing” property will enable us to formulate a geometrical condition for the onset of abrupt bifurcation.

Now, let us briefly investigate the case of particle energies below the hilltop maximum, $E < E_m$. The particle is then excluded from the region $V(x,y) > E$, and, in particular, cannot reach the hill maximum. In this case, for the proper value of b the deflection angle at $y=-y_{\text{end}}$ is π (i.e., there is complete backscattering which is not possible for $E=E_m+0^+$ where the maximum deflection angle is $\pi/2+\theta$). Thus, when passing through E_m , a sudden change occurs in the scattering process and, simultaneously, also in the topology of the energy surface [i.e., (x,y) values in $E_m \geq V(x,y) > E$ are excluded]. Figure 5 shows the deflection function obtained for $\Delta E=E_m-E=0.1$. In order to avoid strong overlap of the graphs we have plotted ϕ as a function of b rather than of δ . One clearly sees that the absolute maximum is at $\phi=\pi$. When β increases, $\phi(b)$ becomes more and more asymmetric and develops an increasing average slope to the left of its maximum. An analytic computation based on the form of the trajectories given above shows, however, that $\phi(b)$ is always continuous for $E < E_m$ (i.e., what we observe is a rapid change but not a jump).

III. THE CONDITION FOR A LOCAL MAXIMUM IN THE DEFLECTION ANGLE

A simple geometrical sufficient condition for abrupt bifurcation can only be found if there is no local maximum lying above $\pi/2-\theta$ in the deflection function at $E=E_m+0^+$. A local maximum value would necessarily depend on details like the actual value of the impact parameter and the incident angle. The condition for the non-existence of a local maximum larger than $\pi/2-\theta$ can be derived from a singularity analysis of $\phi(\delta)$ at $E=E_m$ that we carry out in what follows.

Because of energy conservation, the x -component of the velocity can be given at $E=E_m$ as

$$v_{0x}^2 = (x_0^2 + \beta^2 y_0^2) \cos^2 \theta \quad (11)$$

which in view of Eq. (3) is a unique function of the impact parameter b . Let us first determine the critical impact parameter b_c . Since the critical trajectory does not go to infinity, the coefficient of the terms $\exp(t)$ or $\exp(\beta t)$ must vanish and, thus, we have $A=C=0$. From Eq. (5) it then follows that

$$y_0 = x_0 (\tan \theta) / \beta. \quad (12)$$

By inserting this into the parametrized form Eq. (3) of the initial line, we obtain the critical impact parameter as

$$b_c = -\frac{R}{\cos^2 \gamma} \frac{\beta}{\beta \tan \gamma + \tan \theta}. \quad (13)$$

As long as $\tan \gamma > -(\tan \theta) / \beta$, which we assume in what follows, the critical impact parameter is negative.

Next, let us investigate a small neighborhood of the critical impact parameter $|\delta| \ll 1$. The initial coordinates are then given by

$$x_0 = (b_c + \delta) \cos \gamma \quad (14)$$

and

$$y_0 = b_c (\cos \gamma) (\tan \theta) / \beta - \delta \sin \gamma, \quad (15)$$

respectively. After inserting this into Eq. (11), we find for the initial velocity component

$$v_{0x} = -b_c \cos \gamma \left(1 + \frac{\delta}{b_c} (\cos^2 \theta) (1 - \beta (\tan \gamma) \tan \theta) \right). \quad (16)$$

Consequently, for the coefficients in Eq. (5) we obtain

$$A = C\beta / \tan \theta = (\delta/4) (\cos \gamma) (\sin 2\theta) (\tan \theta + \beta \tan \gamma), \quad (17)$$

$$B = D\beta / \tan \theta = b_c \cos \gamma. \quad (18)$$

Thus, A and C depend linearly on δ , while B and D are constant in leading order. The quantity z defined by Eq. (8) taken at $\mp y_{\text{end}}$ is, therefore, approximately $\mp y_{\text{end}} / C$ where the sign is determined by that of δ . This implies inverse proportionality to $|\delta|$. The factor z appears [see Eq. (9)] in the form of $Az^{1/\beta}$ which is proportional to $|\delta|^{1-1/\beta}$. The key observation is that, because the other term $Bz^{-1/\beta} \sim |\delta|^{1/\beta}$, the complete denominator in Eq. (9) is small and the argument of the arctan function is thus

diverging. By using the approximate formula $\arctan u \approx \pi/2 - 1/u$ valid for $u \gg 1$, we obtain for the deflection function [Eqs. (9) and (10)] after substitution

$$\phi(\delta) = \left| \mp \frac{\pi}{2} - \theta + (\tan \theta) \left(w \frac{|\delta|}{y_{\text{end}}} \right)^{1-1/\beta} \pm \frac{R \cos^2 \theta}{y_{\text{end}} 2\beta w} \left(w \frac{|\delta|}{y_{\text{end}}} \right)^{1/\beta} \right| \quad (19)$$

where

$$w = \frac{(\cos \gamma)(\cos^2 \theta)}{2\beta} (\tan \theta + \beta \tan \gamma) \quad (20)$$

and the upper sign corresponds to positive δ .

This formula shows that there is an important qualitative change in the small δ behavior at $\beta=2$ since for $\beta < 2$ the first power dominates, while for $\beta > 2$ the second one. In the case of backscattering ($\delta > 0$) this does not imply a drastic change in the shape of $\phi(\delta)$ since both terms are of the same sign (remember, θ and $\tan \theta + \beta \tan \gamma$ are positive): $\phi(\delta)$ decreases monotonically with increasing δ as pointed out in the previous section. For forward scattering ($\delta < 0$), however, the difference between the cases with $\beta < 2$ and $\beta > 2$ is striking. As long as $\beta < 2$, $\phi(\delta)$ always starts to grow with $|\delta|$ since the dominating term being proportional to $\delta^{1-(1/\beta)}$ has a positive sign. Since $\phi(\delta)$ must decrease for large values of the impact parameter, this implies the existence of a local maximum at some negative δ . For $\beta > 2$ the situation is different since the other power with negative sign dominates for $\delta \rightarrow 0$ and, consequently, $\phi(\delta)$ starts to decrease when moving away from the origin in the negative δ range but with δ still very small in the modulus.

The case $\beta=2$ is a borderline situation when both powers $1-1/\beta$ and β are the same. The coefficients of the two terms are, however, of different signs. Consequently, there exists a critical angle θ_c so that for incident angles greater (smaller) than θ_c the deflection function increases (decreases) when δ starts to grow in the negative direction. By equating the coefficients of the two powers, the following equation is obtained for θ_c

$$\frac{R}{y_{\text{end}}} = (\cos \gamma)(\tan \theta_c)(\tan \theta_c + 2 \tan \gamma) \quad (21)$$

with the solution

$$\tan \theta_c = \left(\tan^2 \gamma + \frac{R}{y_{\text{end}}} (\tan^2 \gamma + 1)^{1/2} \right)^{1/2} - \tan \gamma. \quad (22)$$

For initial lines running parallel to the x -axis ($\gamma=0$) $\tan \theta_c = (R/y_{\text{end}})^{1/2}$. In the particular case of our plots $R=y_{\text{end}}$, the critical angle is just $\theta_c = \pi/4$. In the general case, the dependence of the critical angle on γ and R/y_{end} can be seen in Fig. 6.

Interestingly, the properties of the deflection function discussed above do not exclude the existence of a local maximum close to the origin even in the case $\beta > 2$. The reason is that the next to leading term with power $1-1/\beta$ might be of the same order as the leading one at still small

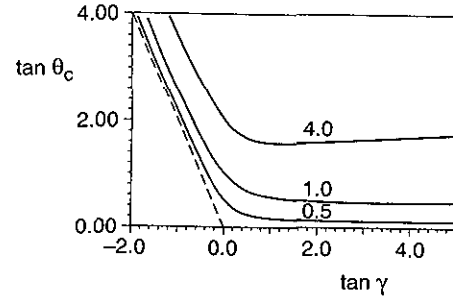


FIG. 6. Dependence of the critical angle θ_c on the slope γ of the initial line at different geometrical ratios R/y_{end} (indicated above the curves) as obtained from Eq. (22). The dashed line is the left asymptote $\tan \theta_c = -2 \tan \gamma$ to all of the curves.

values of δ especially if β is close to 2. These two terms might fully compensate each other at some critical δ_c for $\beta > 2$ where

$$\frac{\delta_c}{y_{\text{end}}} = - \frac{y_{\text{end}} 2\beta \sin \theta}{R \cos^3 \theta} \left(\frac{R \cos^3 \theta}{y_{\text{end}} 2\beta w \sin \theta} \right)^{(2\beta-2)/(\beta-2)} \quad (23)$$

and w has been defined by Eq. (20). The value of the big parentheses is smaller (greater) than unity for $\theta > \theta_c$ ($\theta < \theta_c$) for β around 2. This shows that for $\theta > \theta_c$ a critical impact parameter δ_c exists around the origin. Consequently, the deflection function is locally increasing for $\delta < \delta_c$ even if $\beta > 2$ and thus a local maximum larger than $\pi/2 - \theta$ can exist at a finite distance from the origin [see, e.g., Fig. 4(c) for $\beta=2.25, 2.5$]. For $\theta < \theta_c$, however, δ_c defined by Eq. (23) is never small. Consequently, the value of the deflection function is always smaller than $\pi/2 - \theta$ in the region of validity ($|\delta| \ll 1$) of our approximation. Numerics show that the lack of a local maximum lying above $\pi/2 - \theta$ remains valid in a range of order unity away from the origin. Thus, scatterings with trajectories ending in the half-plane $x > 0$ occur if the incident angle is smaller than θ_c and $\beta > 2$.

IV. GEOMETRICAL SUFFICIENT CONDITION FOR ABRUPT BIFURCATION IN SCATTERING ON AN ELLIPTICALLY SHAPED HILL OF FINITE HEIGHT

We choose here a simple example, the scattering from three isolated hills $V(x,y) = V_1(x,y) + V_2(x,y) + V_3(x,y)$, where hill 1 is of the form

$$V_1(x,y) = \begin{cases} E_{m_1} - (x^2 + \beta^2 y^2)/2 & \text{if } x^2 + \beta^2 y^2 \leq 2E_{m_1}, \\ 0 & \text{otherwise,} \end{cases} \quad (24)$$

with $E_{m_1} > 0$. We assume that hills 2 and 3 also have non-zero potentials only in regions of finite extent. In what follows we shall show that for $\beta > 2$ an abrupt bifurcation to chaotic scattering occurs as E is reduced through the maximum potential of hill 1 provided that hills 2 and 3 are located inside the wedge shown in Fig. 7, where θ_c is derived below [see Eq. (32)]. [We emphasize that the above simple geometrical condition is only a *sufficient* condition

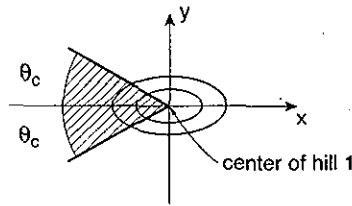


FIG. 7. Geometrical sufficient condition for abrupt bifurcation. If hills 2 and 3 lie in the shaded region $|\theta| < \theta_c = 38^\circ 10'$, an abrupt bifurcation occurs.

for an abrupt bifurcation, and that abrupt bifurcations may still occur even if this condition does not hold (see Sec. V).]

To obtain this result depicted in Fig. 7, we first note that, under our assumed condition, the size of the regions where $V_{1,2,3}(x,y) \neq 0$ is small relative to the distances between the hills, and that the separation distances between the three hills is much greater than the extent of their regions of nonzero potential. Furthermore we assume that the maxima of both $V_2(x,y)$ and $V_3(x,y)$ exceed the particle energy E and that, whatever the form of the potentials $V_2(x,y)$ and $V_3(x,y)$, the dynamics in the absence of hill 1 is nonchaotic [i.e., for $E_{m_1} = 0$, $V(x,y)$ has no chaotic orbits]. The essential deflection process from hill 1 can be studied by starting trajectories on a line outside the boundary contour $x^2 + \beta^2 y^2 = 2E_{m_1} \equiv C_0$, as depicted in Fig. 8. The initial coordinates are parametrized with the distance s measured along the line which is assumed to be perpendicular to the initial velocities.

The motion is free before the trajectory reaches the outermost contour of the hill. After this the trajectory can

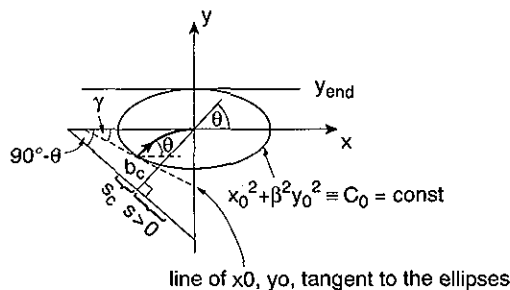


FIG. 8. Diagram illustrating scattering trajectories in the case of an elliptically shaped potential hill of finite size at $E = E_{m_1} + 0^+$. The outermost contour is the isopotential line with energy zero and is given by $x^2 + \beta^2 y^2 = 2E_{m_1} \equiv C_0 = \text{const}$. Trajectories are launched toward the hill along a straight line making an angle of $\pi/2 - \theta$ with the x -axis under inclination angle θ so that the line does not cross the outermost contour. The impact parameter s is the distance of the initial point measured along this line from its closest point to the origin. $s_c < 0$ denotes the impact parameter of the critical trajectory. The dashed line is tangent to the outermost contour at the point where the critical trajectory enters the region of nonzero potential. Its slope γ is uniquely determined by the inclination angle θ (see text). Trajectories lying close to the critical one can equally well be described as if they started on the dashed line with initial coordinates x_0, y_0 and moved in an infinitely extended potential until reaching the line $y = \pm y_{\text{end}} = \pm C_0^{1/2}/\beta$. Therefore, the results of the singularity analysis of Sec. III are also applicable to the present problem.

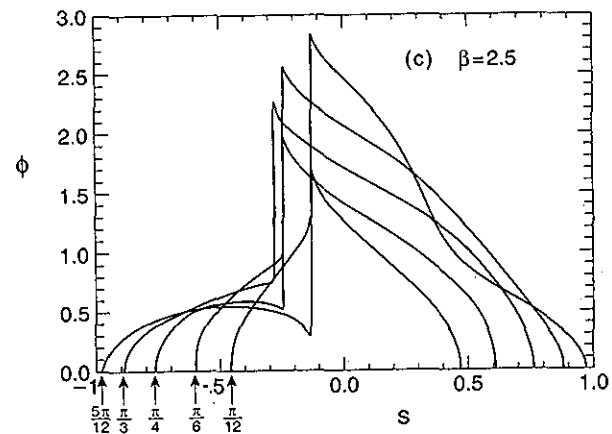
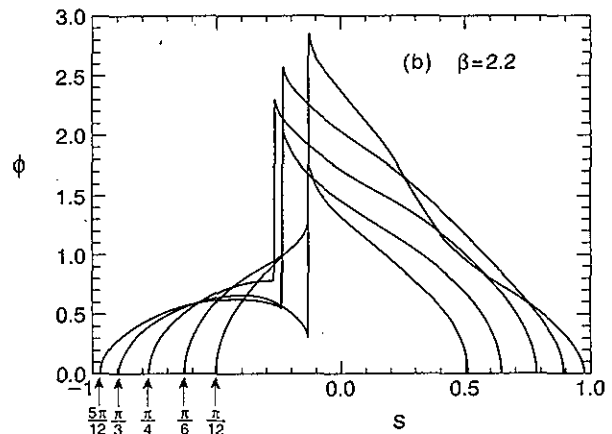
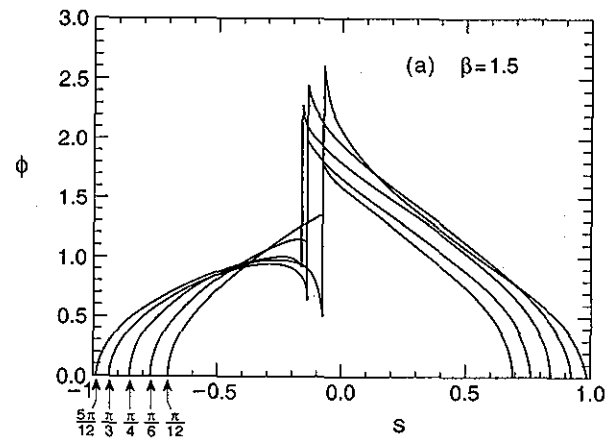


FIG. 9. Deflection function $\phi(s)$ of elliptically shaped potential hills of finite heights at $E = E_{m_1} + 0^+$ as obtained from Eqs. (9) and (10) by numerically determining the point of exit on the outermost contour. Different inclination angles $\theta = \pi/12, \pi/6, \dots, 5\pi/12$ are taken at elongation parameters $\beta = 1.5$ (a), $\beta = 2.2$ (b), and $\beta = 2.5$ (c). The initial line is the same as in Fig. 4.

be computed in the same way as for the infinite potential and the deflection angle ϕ is determined by the particle velocity when the trajectory crosses the outermost contour again. The computation of this point requires the solution of an implicit equation which can be easily done numerically.

The results obtained for $E = E_{m_1} + 0^+$ at different β

values and incident angles are shown in Fig. 9. Qualitatively they exhibit very much the same features as the deflection on an infinite hill but strongly compressed along the s -axis. We observe again that for θ less than some critical value, which will be determined analytically below, no local maxima larger than $\pi/2 - \theta$ are created as long as $\beta > 2$. The deep decrease at certain positive values of s is a remnant of the singularity generated in the case of infinitely extended potentials by trajectories escaping parallel to the x -axis. Because of the finite extension of the potential the singularity cannot be built up now and, consequently, the derivative of the deflection function is finite for positive s . The jump from a deflection angle of $\pi/2 - \theta$ to $\pi/2 + \theta$ is connected again with a critical trajectory that reaches the hilltop in an infinitely long time.

The critical s -value s_c can be determined as follows. Any trajectory started at s along the line shown in Fig. 8 has the form

$$y = x \tan \theta - s / \cos \theta \tag{25}$$

in the force-free region. The point (x_0, y_0) where the trajectory enters the region of finite force is then obtained as the intersection of this straight line with the outermost contour $x^2 + \beta^2 y^2 = 2(E_{m_1} - E_0) \equiv C_0$. The critical value s_c can again be computed from the fact that for such a trajectory $A = C = 0$. Since inside the contour Eq. (5) holds, we conclude that $x_0 = -v_{0x}, y_0 = -v_{0y}/\beta$ must be fulfilled with

$$v_{0x} = C_0^{1/2} \cos \theta. \tag{26}$$

Consequently, we find that

$$s_c = - \left(1 - \frac{1}{\beta} \right) \frac{1}{2} C_0^{1/2} \sin (2\theta). \tag{27}$$

The form of the deflection function $\phi(s)$ around the critical value as a function of $\delta' = s - s_c$ can be derived from the results of the previous section. From the point of view of singularity analysis, the finite hill case corresponds to a situation of the infinite hill problem when the line of x_0, y_0 is just tangent at b_c to a given contour, and the lines $y = \pm y_{\text{end}}$ exactly touch the *same* contour (the impact parameter b is measured again from the intersection with the y -axis). This means that

$$C_0 = x_{0c}^2 + \beta^2 y_{0c}^2 \text{ and } y_{\text{end}} = C_0^{1/2} / \beta, \tag{28}$$

where x_{0c} and y_{0c} denote the coordinates of the critical trajectory along the x_0, y_0 -line. A simple geometrical observation yields $x_{0c} = b_c \cos \gamma$ and $R = -(y_{0c} + b_c \sin \gamma) \cos \gamma$ where R is the distance of the x_0, y_0 -line from the origin. Using Eq. (13) which connects R and b_c , we find that y_{0c} and b_c are related as $y_{0c} = b_c (\cos \gamma) (\tan \theta) / \beta$. By computing the slope of the tangent to the ellipses at x_{0c}, y_{0c} we immediately find that the angles γ and θ fulfill the following basic relation:

$$\tan \gamma = \frac{1}{\beta \tan \theta}. \tag{29}$$

Since the line of initial condition in the force-free region and the line containing x_0, y_0 cross each other under an

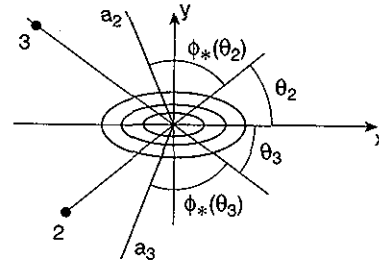


FIG. 10. Diagram illustrating the selection of configurations (θ_2, θ_3) with abrupt bifurcation even if the geometrical sufficient condition of Fig. 7 does not hold (see text).

angle $\pi/2 - \theta - \gamma$, the deviation from the critical values, δ and δ' are connected by $\delta' = \delta \sin (\gamma + \theta)$ which in view of Eq. (29) reads as

$$\delta' = \frac{\cos \theta}{(1 + \beta^2 \tan^2 \theta)^{1/2}} (1 + \beta \tan^2 \theta) \delta. \tag{30}$$

By substituting this into Eqs. (19) and (20), we can obtain the form of $\phi(\delta')$ valid in the limit $\delta' \ll 1$.

We can thus also take over the results obtained for the critical angle θ_c and apply it to the case of finite hill. In particular, because of Eqs. (28) and (29) we find that

$$\frac{R}{y_{\text{end}}} = \frac{\cos \gamma}{\sin \theta}. \tag{31}$$

A substitution of this into Eq. (22) taken at $\beta = 2$ leads to $\cos^2 \theta_c = \sin \theta_c$ which is solved by

$$\theta_c = \arcsin \left(\frac{\sqrt{5} - 1}{2} \right) \approx 38^\circ 10'. \tag{32}$$

Note that θ_c is a kind of “golden” angle. This result also shows that the critical angle in the case of finite hills is more universal than for infinitely extended hills as it does not depend at all on the choice of initial conditions.

V. NONGEOMETRICAL CONDITIONS

The local maximum value $\phi_*(\theta)$ of the deflection function at a given incident angle θ (and β fixed) can easily be read off from plots like Fig. 9 obtained for given potential shapes. The condition for abrupt bifurcation can then be worked out easily. For potentials of the form $V(x, y) = V_1(x, y) + V_2(x, y) + V_3(x, y)$ with V_1 as given by Eq. (24) this can be done as follows. Let us denote the angle between the position vector of hill 2 and the x -axis by θ_2 . Draw a line under angle $\theta_2 + \phi_*(\theta_2)$ to the x -axis (line a_2 in Fig. 10). Trajectories coming from hill 2 with energy $E = E_{m_1} + 0^+$ will then not be reflected toward hill 3 if the latter lies in the lower left of the boundary determined by line a_2 and the negative y -axis (see Fig. 10). Next, position hill 3 in this region. Check, by applying the same procedure, to see if deflection of trajectories coming from hill 3 by hill 1 toward hill 2 is possible at $E = E_{m_1} + 0^+$, i.e., if hill 3 lies to the upper left of line a_3 and the positive y -axis. If the answer is positive, we say that the pair (θ_2, θ_3) defines a configuration with abrupt bifurcation. We consider con-

TABLE I. The height $\phi_*(\theta)$ of the local maximum of the deflection function measured relative to the deflection angle $\pi/2 - \theta$ of a trajectory approaching the critical one from the left for the isolated potential defined by Eq. (24). The values $\phi_*(\theta) + \theta - 90^\circ$ are listed as read off from Fig. 9, angles are given in degrees. The table contains a zero if no local maximum above $\pi/2 - \theta$ exists.

β	θ				
	15	30	45	60	75
1.5	1	6	12	24	38
2.2	0	0	0	7	19
2.5	0	0	0	4	16.5

figurations where θ_2 and θ_3 are of different sign which means that one of the hills lies above the x -axis, the other one below, and in what follows only the modulus of θ_2 and θ_3 will be given.

The values of ϕ_* can easily be extracted from the graphs of Fig. 9. In Table I we listed $\phi_*(\theta) - (\pi/2 - \theta)$, i.e., the angle between the line a_2 or a_3 and the y -axis for a few incident angles θ and elongation parameter β . If no local maximum exists above $\pi/2 - \theta$, the table contains a zero. We thus find that for $\beta = 1.5$ abrupt bifurcation occurs in the model for the configurations $(\pi/12, \pi/12), \dots, (\pi/12, 5\pi/12), (\pi/6, \pi/6), \dots, (\pi/6, 5\pi/12), (\pi/4, \pi/4), (\pi/4, \pi/3), (\pi/4, 5\pi/12)$, and $(\pi/6, \pi/6)$. If $\beta > 2$, we know that cases with $\theta_2, \theta_3 < \theta_c$ are necessarily accompanied with abrupt bifurcation. Although $\pi/4 > \theta_c$, the plot of the deflection function shows [see Figs. 9(b) and 9(c)] that at this incident angle there is no local maximum lying above $\pi/2 - \theta$ if β is not very close to 2, like e.g. for $\beta = 2.2, 2.5$. This observation shows that the actual range of abrupt bifurcation might turn out to be much larger in particular cases than the one given by the geometrical condition. In fact, it follows from Table I that the configurations $(\pi/4, \pi/4), (\pi/4, \pi/3), (\pi/4, 5\pi/12)$, and even $(\pi/3, 5\pi/12)$ are allowed for abrupt bifurcations for both $\beta = 2.2$ and $\beta = 2.5$. We thus conclude that there are entire continua of (θ_2, θ_3) for any elliptical hill where abrupt bifurcation can occur. These events are, therefore, typical in potential scattering.

We can also see from Table I that the value of $\phi_*(\theta)$ decreases with increasing β . In the limit $\beta \gg 1$ we expect ϕ_* to go to $\pi/2 - \theta$, i.e., the local maximum in ϕ to disappear. Thus, for an extremely elongated hill 1 abrupt bifurcation is expected to occur in all cases when the other hills both lie on the left or on the right of the line defined by the minor semiaxis.

VI. CONCLUSIONS

The abrupt bifurcation to chaotic scattering was introduced in Ref. 5 and was illustrated there primarily for the case of isolated potential hills with locally circular isopotential contours at the hilltops. The object of this paper has been to illustrate the effect of noncircularity. It is found that abrupt bifurcations still occur in the noncircular case, but that major changes in the phenomenon result as soon

as there is any deviation from circularity (i.e., the circular case is singular). We have considered the case of three isolated potential hills that are widely separated compared to their individual spatial extents. For the example of the case where the hill of lowest hilltop potential is given by $V_1(x, y) = E_{m_1} - (x^2 + \beta^2 y^2)/2$ for $E_{m_1} \geq (x^2 + \beta^2 y^2)/2$, and $V_1(x, y) = 0$ otherwise, we show how to obtain explicit conditions for when an abrupt bifurcation occurs. One of these results is a simple geometrical sufficient condition for the existence of an abrupt bifurcation. This condition is illustrated in Fig. 7. In Fig. 7 we show the potential contours of the hill with lowest hilltop energy (hill 1). If the ellipticity parameter β exceeds two, and if hills 2 and 3 are located in the shaded wedge of angular width $2\theta_c$, where θ_c is given by Eq. (32), then an abrupt bifurcation occurs as the particle energy is lowered through the hilltop potential E_{m_1} . Based on this example and on the case of the infinitely extended elliptical hill, we think that a critical θ_c can also be found for potentials which are only locally elliptically shaped and sufficiently elongated. In cases when the sufficient geometrical condition does not hold (e.g., $\beta < 2$) abrupt bifurcation can also occur, but a more detailed analysis is necessary to determine whether the onset of chaotic scattering is abrupt. An illustration of how to do this for our example is given in Sec. V. To conclude we re-emphasize the point made in the introduction: knowledge that a bifurcation to chaotic scattering is abrupt gives important information with respect to the dynamics and its evolution with parameter variation. In particular, there is a characteristic variation of the stability of the chaotic set, and since it is hyperbolic at creation, there are no bifurcations creating periodic orbits or KAM surfaces in a parameter interval starting at the point of the abrupt bifurcation.

ACKNOWLEDGMENTS

This research has been supported by the Hungarian Science Foundation under Grant Nos. OTKA 2090 and OTKA T4439, by the U.S.-Hungarian Science and Technology Joint Fund in cooperation with the NSF and the Hungarian Academy of Sciences under Project 286, by the Office of Naval Research (Physics), and by the U.S. Department of Energy (Office of Scientific Computing, Office of Energy Research).

- ¹U. Smilansky, in *Chaos and Quantum Physics*, edited by M. Giannoni, A. Voros, and J. Zinn-Justin (North-Holland, Amsterdam, 1992).
- ²C. Jung, *Acta Phys. Polonica* **23**, 177 (1992).
- ³R. Blümel, in *Directions in Chaos*, edited by D. H. Feng and J.-M. Yuan (World Scientific, Singapore, 1992), Vol. 4.
- ⁴J. F. Heagy, Z.-M. Lu, J.-M. Yuan, and M. Vallieres, in Ref. 3.
- ⁵(a) S. Bleher, C. Grebogi, and E. Ott, *Phys. Rev. Lett.* **63**, 919 (1989); (b) *Physica D* **46**, 87 (1990).
- ⁶M. Ding, C. Grebogi, E. Ott, and J. Yorke, *Phys. Rev. A* **42**, 7025 (1990).
- ⁷M. Ding, C. Grebogi, E. Ott, and J. Yorke, *Phys. Lett. A* **153**, 21 (1991).
- ⁸M. Ding, *Phys. Rev. A* **46**, 6247 (1992).
- ⁹T. Tél, *Phys. Rev. A* **44**, 1034 (1991).
- ¹⁰P. Cvitanovic and B. Eckhardt, *Phys. Rev. Lett.* **63**, 823 (1989).
- ¹¹T. Tél, *J. Phys. A* **22**, L691 (1989).
- ¹²Z. Kovács and T. Tél, *Phys. Rev. Lett.* **64**, 1617 (1990).